„Tailoring of hydrothermally altered diatomite for the removal of metal ions from waste water“

Bachelor thesis
by
Gerald Raab

Institute of Applied Geosciences
Mineralogy & Hydrogeochemistry

Advisors:
Univ.-Prof. Dipl.-Min. Dr.rer.nat. Martin Dietzel
Dipl.-Min. Daniel Höllen

August 2012

Statement of Originality

This thesis contains no material that has been accepted for the award of any other degree or diploma in any other university. To the best of my knowledge, this thesis contains no material previously published or written by another person, except where reference is made in the text.

17/08/12 Gerald Raab

Abstract

One of the fields of research on the Graz University of Technology at the Institute of Applied Geosciences is waste water treatment. One aspect is to create a proper material which has a high ion exchange capacity to remove e.g. heavy metals from aqueous solutions. This thesis is dealing with alteration products synthesized from diatomite at 100 °C using 0.1 M KOH with and without Al^{3+}. The overall task of the present study is to obtain alteration products which can be used to remove dissolved heavy metal ions for waste water treatment issues. Diatomite from a northern African deposit was used for the hydrothermal treatment. The metal removal experiments were performed with a mine drainage solution and a synthetic Cu^{2+}, Pb^{2+}, and Zn^{2+} ion bearing solution.

Through hydrothermally alteration the pH and the concentration of dissolved K^{+} and Al^{3+} decrease whereas the concentration of dissolved silica increases in the experimental solutions. The SEM imaging revealed etching effects at the diatomite surface. The XRD patterns indicate no crystalline phase except detrital quartz and illite. This surface alterations may be predominantly related to the formation of an amorphous material. This solid phase can be considered as an “intermediate phase” (IP). It appears that Al^{3+} stabilizes the IP, because after 6 days of hydrothermal treatment without Al^{3+} the IP disappears continuously.

The analyses of dissolved metal ions after metal removal experiments display the selectivity order of Pb^{2+} > Cu^{2+} > Zn^{2+} and a significant increase of the metal removal capacity for materials hydrothermally treated versus the unaltered diatomite. The diatomite treated in the presence of Al^{3+} is more capable of removing metal ions from the synthetic metal bearing solution, while the diatomite altered without Al^{3+} yield a better performance with respect to the mine drainage solution.

Contents

1 Introduction....5
1.1 Occurrence and structure of zeolites....5
1.1.1 Synthesis of zeolites....6
1.1.2 Utilization....6
1.2 Diatoms....6
2 Materials and Methods....7
2.1 Materials....7
2.1.1 Diatomite....7
2.1.2 Aqueous solutions....7
2.2 Analytical Methods....8
2.2.1 pH....8
2.2.2 Scanning electron microscopy....8
2.2.3 X-ray diffraction....9
2.2.4 Inductively coupled plasma optical emission spectrometry....9
2.2.5 Inductively coupled plasma mass spectrometry....10
3 Experiment Design....12
3.1 Alteration experiments....12
3.2 Metal removal experiments....14
4 Results....16
4.1 Alteration experiments....16
4.1.1 Solution chemistry....16
4.1.2 Alteration product....17
4.1.3 Mineralogical changes of the diatomite....21
4.2 Metal removal experiments....22
4.2.1 Synthetic metal ion solution....22
4.2.2 Mine drainage solution....23
4.2.3 Evolution of pH through ion exchange experiments....24
5 Discussion....25
6 Conclusions....26
Literature....27

1 Introduction

Diatoms are siliceous algae which have a wide range of industrial applications due to their porous structure, e.g. for the removal of particular contaminants from waste waters ***(Smol&Stoermer, 2010)***. Zeolites are hydrous framework silicate which can be applied for removal of dissolved metal ions from contaminated water ***(Motsi, Rowson&Simmons, 2009)***. Therefore it is desirable to combine these two properties by tailoring a proper composite material. The aim of the present thesis is the transformation of diatomite to such kind of material by hydrothermal treatment. Therefore a synthesis at 100 °C using 0.1 M KOH with and without additional Al^{3+} over several intervals were performed. The reaction products were used for metal removal experiments to prove their suitability for waste water treatment.

1.1 Occurrence and structure of zeolites

Zeolites are hydrous framework silicates which occur predominantly in metamorphic rocks. They form at low pressure and low temperature and are eponymous for the zeolite facies. Zeolites are also formed in young volcanic rocks like basalts and phonolites, where they partly fill up hollow spaces and fissures or are the result of a conversion of rock glass or volcanic tuff. They can also be found on oceanic sea floors close to hydrothermal vents like black smokers and in continental salt lakes. The name itself is form the Greek ζέω (*zéō*) and λίθος (*líthos*), which can be translated as “boiling stone”. It is based on the ability to adsorb a large amount of water, also called zeolite-water, without affecting the stability of the crystal structure which is characterized by cavities and channels containing not only H_2O molecules but also exchangeable cations ***(Okrusch&Matthes, 2009).*** Zeolites can be defined as minerals containing more than 50 % of silicon and aluminium and possessing a framework of tetrahedrons, with only 20 or less tetrahedral atoms per 1000 Å³ (cubic Ångstrom). The cavities are connected and contain cations and water molecules ***(Bish&Ming, 2001).*** The general formula $M_xD_y[Al_{x+2y}Si_{n-(x+2y)}O_{2n}]\cdot mH_2O$ comprises a M-position for all monovalent cations, a D-position for all divalent cations, which neutralise the negatively charged framework in the square bracket. The water molecules mostly just hydrate the cations in the cavities ***(Bish&Ming, 2001).***

1.1.1 Synthesis of zeolites

The development of the zeolite synthesis started in the mid-20th century. Most of the commercial zeolites are hydrothermally synthesized. An aqueous mixture of silicon and aluminium compounds is prepared and alkali metal cations are added. Often organic templates are used. The properties of the reaction products are influenced by e.g. solution composition, temperature and reaction time. Because of the thermal activation of the process, the heating method plays a critical role, especially the heating rate and the temperature gradient in the reaction mixture ***(Jawor, Jeong&Hoek, 2009).***

1.1.2 Utilization

Zeolites possess a wide range of applications in industry, agriculture, construction and also in domestic homes. Because of the cavities zeolites possess a high inner surface (up to 1000 m^2g^{-1}) which results in an enormous cation exchange capacity. For instance zeolites are used for fixation of Ca^{2+}-ions from water by replacing Na^{+}-ions in their crystal structure. Afterwards the calcium rich zeolite can be renewed by back-exchange with Na^{+}-containing solutions. A second example is the separation of molecules and gases (in particular noble gases) by size due to the well defined diameter of the cavities of the – mostly drained – zeolites ***(Okrusch&Matthes, 2009).***

1.2 Diatoms

“Diatoms are unicellular algae that are characterized by an external two-part skeleton called a frustule of opaline silica. Frustules are commonly very intricate and variable, and the patterns and types of ornamentation of the frustule form the basis of nearly all diatom taxonom.“ ***(Lipps, 1993).*** The frustule consists of two valves or theca which differ slightly in size. Both have a valve plate and cingulum. The smaller valves, the hypotheca, fits into the larger one or epitheca in such a way that one cingulum overlaps the other, forming a connective band or girdle ***(Bignot, 1985).*** „The size of diatom frustules ranges from less than 1 µm to more than 1000 µm, but most frustules range in size from 10 to 100 µm” ***(Lipps, 1993).*** When diatoms die they sink down to the ocean floor and their inorganic parts form sediments, so-called diatomite. There are three major belts of diatomaceous sediments. One is circling the globe between 45° and 65° south, one belt in the north within the Pacific including the Sea of Okhotsk, Sea of Japan, Bering Sea and in the Atlantic developed somewhat in the Norwegian Sea. The last belt is an equatorial belt which is well defined in the Pacific and the Indian Oceans but less well defined in the Atlantic Ocean ***(Lipps, 1993).***

2 Materials and Methods

2.1 Materials

2.1.1 Diatomite

The diatomite used in this study originates from a northern African deposit (Thiele) and contains predominantly diatoms of the *Centrales* group. The diatomite has a specific BET surface area of 12.6 m^2g^{-1} and consists of 97 wt-% amorphous phase (opaline cell walls), 2 wt-% mica and 1 wt-% quartz. Its chemical composition is 93.3 wt-% SiO_2, 1.7 wt-% Al_2O_3, 0.8 wt-% Fe_2O_3, 0.2 wt-% MgO, 0.3 wt-% CaO, 0.3 wt-% K_2O and 3.5 % L.O.I. (***Höllen, 2012***).

2.1.2 Aqueous solutions

For the hydrothermal synthesis 0.1 M KOH was prepared by dissolving 2.79 g KOH pellets (Merck p.a.) in 500 ml MilliQ water resulting in a pH of 12.9. Two different sets of experiments were performed:

a) Experiments with Al^{3+}: 1.008 g gibbsite (γ-$Al(OH)_3$ were suspended in 0.1 M KOH in a gas-tight Nalgene® polycarbonate bottle to prevent CO_2 absorption and stirred with a magnetic stirrer for one week at 50 °C and separated from the partly remaining gibbsite by membrane filtration (0.45 µm). The resulting solution contained 11 mM of Al^{3+} mostly as $Al(OH)_4^-$ at pH 12.8, which represents still undersaturation with respect to gibbsite (saturation index: $SI_{gibbsite}$ = -0.33 at 25 °C; PHREEQC with database PhreeqC (***Parkhurst&Apello, 1999***)). Since the solubility of gibbsite and amorphous aluminium hydroxide increases with temperature, no precipitation of $Al(OH)_3$ is expected by heating of the “pure” stock solution.

b) Experiments without Al^{3+}: 0.1 M KOH was used for alteration of diatomite without further treatment.

For the metal removal experiments two different solutions were used:

1) A mine drainage solution (pH 8) from a carbonate-hosted lead-zinc deposit from the Nötschbach creek in Bad Bleiberg (Carinthia). The solution was filtrated and stored at room temperature. The chemical composition of this solution is 1250 $\mu molL^{-1}$ of Ca^{2+}, 665 $\mu molL^{-1}$ of Mg^{2+}, 152 $\mu molL^{-1}$ of Na^{+}, 31 $\mu molL^{-1}$ of $Si(OH_4)$, 26 $\mu molL^{-1}$ of K^{+}, 17 $\mu molL^{-1}$ of Zn^{2+}, 0.014 $\mu molL^{-1}$ of Cd^{2+}, 0.62 $\mu molL^{-1}$ of Sr^{2+} and 0.48 $\mu molL^{-1}$ of Pb^{2+}.

2) For the synthetic solution experiment a stock solution (100 mL MilliQ water, 166.6 mg $Pb(NO_3)_2$, 131.9 mg $Zn(NO_3)_2$ and 122,2 mg of $Cu(NO_3)_2$) was made from $Pb(NO_3)_2$, $Zn(NO_3)_2$ $4H_2O$, $Cu(NO_3)_2$ 3 H_2O, (Merck p.a.) and MilliQ water. The stock solution was diluted 1:10 to a synthetic solution containing 524 $mmolL^{-1}$ of Cu^{2+}, 507 $mmolL^{-1}$ of Pb^{2+} and 515 $mmolL^{-1}$ of Zn^{2+}. The pH of this solution was 5.0 in consistence with PhreeqC modelling using the PhreeqC database ***(Parkhurst&Apello, 1999).***

2.2 Analytical Methods

2.2.1 pH

The pH is defined by the negative logarithm of the hydroniumion activity $pH=-\log_{10}(H_3O)$ ***(Brown, LeMay&Bursten, 2011).*** The pH was measured using WTW Inolab 740 combined with pH electrode BL 26 (Schott). The calibration was performed with three buffer solutions (pH 4, 7 and 10).

2.2.2 Scanning electron microscopy

Scanning electron microscopy (SEM) yields images with a very high spatial resolution (< 1 nm). An electron beam is created by an electron gun (e.g.Tungsten filament) inside of an evacuated chamber. It is accelerated and focused by magnetic lenses and scanning coils before it traces over an object and interacts with the sample. During these interactions secondary electrons get dislodged and can be analysed by a secondary electron detector and an image, showing different levels of brightness, is obtained. The secondary electron image is dominated by the topography contrast, but also the phase contrast and charging effects have an influence. To reduce these charging effects, non-conductive samples like diatomite have to be coated by noble metals ***(Goldstein&Newbury, 1997).*** In this study the samples were sputtered by a Edward Pirahi 50L with a Gold-Palladium alloy at 10^{-1} mbar and investigated with the Zeiss DM 982 5 mA and 3-5 kV.

2.2.3 X-ray diffraction

X-ray diffraction (XRD) uses the diffraction of x-rays on the lattice planes of a crystal to obtain information about the crystal structure. The relation between the peak order (n), the wavelength (λ), the angle between x-ray and lattice plane (Θ) and the distance between the lattice planes (d) has been described by William Lawrence Bragg, according to the equation

$$n\lambda = 2d \sin \Theta \quad (1)$$

(Allmann, 2002). From the d-values and the relative intensities of their corresponding peaks crystalline phases can be identified using special databases ***(Allmann, 2002).*** In an x-ray diffractometer a copper, cobalt or molybdenum anode produces an x-ray with a well-defined wavelength. During an x-ray diffraction analysis the angle Θ is changed stepwise. At certain angles the corresponding lattice planes diffract the x-rays to a detector which results in an intensity peak at this d-value or angle. The change of the angle results in a complete x-ray diffraction pattern. In this study a PANalytical X´Pert Pro X-ray spectrometer with Co Kα radiation, a beam current of 40 mA and an acceleration voltage of 45 kV were used. The sample was rotated during the measurement to improve statistics and the diffraction angle was varied between 2Θ of 4° and 110°. The Rietveld refinement approach was applied for quantification (*PANanaytical X´Pert High Score Plus). Zincite (Johnson Matthey, spec. pure) was used as an internal standard for quantification of the amorphous phase. 0.01 g Zinc oxide (zincite) and 0.06 g of the altered samples were mixed to a homogeneous powder with an agate mortar. All initial weights were written down to calculate the exact amount of the identified minerals of the samples afterwards. Scaling factors of the crystalline phases, zero shift and peak-shape parameter were refined in the mentioned order.

2.2.4 Inductively coupled plasma optical emission spectrometry

Inductively coupled plasma optical emission spectrometry (ICP-OES, Perkin Elmer Optima 4300 DV) was used to determine the chemical composition of the solutions from the alteration experiments. The liquid samples are transformed to an aerosol by a nebulizer using argon as a carrier gas. This aerosol enters an argon plasma which is produced by electromagnetic induction with a copper coil. The plasma has a temperature between 6000 and 10000 °C and consists predominantly of positively charged ions and isolated electrons. In the plasma the sample is atomized and ionized to predominantly monovalent species. The plasma is enlightened by a mercury lamp with monochromatic radiation. This radiation excites the electrons to upper energy levels.

Later they relax to a lower level and the energy loss is released as electromagnetic radiation. The wavelength of this radiation which is detected by a photomultiplier corresponds to a certain energy gap which is characteristic for a certain chemical element. The intensity at a certain wavelength correlates with the concentration of the respective element ***(Skoog&Leary, 1996).*** In this study the calibration was performed by a commercial multi-element standard (Merck ICP-MS standard X) and a self-made standard containing 1 mgL^{-1} Si^{4+} and 100 μgL^{-1} Al^{3+}. Each sample was measured five times to receive a mean value and a standard deviation with an measuring accuracy of about 2 %. The intensity was integrated over the central three measuring points of the peak area.

2.2.5 Inductively coupled plasma mass spectrometry

Inductively coupled plasma mass spectrometry (ICP-MS, Agilent 7500 cx) was used to determine the chemical composition of the heavy metal solutions in the ion exchange experiments. The transformation of the sample into the plasma and the formation of the plasma itself are the same as for ICP-OES (2.2.4). But instead of optical excitation of the electrons the ions are separated by their mass:charge ratio in an electromagnetic field. The charged ions are effected by the Lorentz force F according to the equation

$$F = F_E + F_B = q\,(E + vB) \qquad (2)$$

where F_E and F_B are the electric and the magnetic component of the Lorentz force, q is the charge of the ions, v their velocity and B the magnetic field. On the other hand the ions are effected by a gravitational force due to their mass according to Newton´s second law of motion

$$F = ma \qquad (3)$$

stating that a force, F, accelerates a mass, m, to a certain acceleration, a. Equalizing these equations results in

$$(m/Q)a = E + vB \qquad (4)$$

This means that for every mass:charge ratio (m/Q) at given electromagnetic conditions (E and B) and a given velocity of the entering ion, v, the direction of flight is influenced by a certain acceleration, a. This results in separation of the ions according to their mass:charge ratio. It has to be considered that different ions might possess the same mass:charge ratio. This results in so-called interferences.

Fortunately, many elements have different isotopes resulting in different mass:charge ratios. Hence the isotope can be chosen which has the fewest and weakest interferences. **(*Taylor, 2001).*** In this study the calibration was performed by three multi-element standards (10 ngL^{-1}, 10 μgL^{-1}, 10 mgL^{-1}) which were diluted from an Inorganic Ventures IV-ICPMS-71A multi-element standard using supra pure HNO_3 and MilliQ water. Quantification was based on peak height using a linear calibration function with a blank solution (2 % HNO_3) besides the standards. The measuring inaccuracy is about 2 %. The measured masses for each element are given in the results tables.

3 Experiment Design

3.1 Alteration experiments

For both experimental series 0.5 g diatomite were put into Teflon inserts which were placed in steel autoclaves. The autoclaves were labelled with a number. Every number was assigned to a reaction time and a sample code. 25 ml of the respective alkaline solution (with or without Al^{3+}) were placed into the Teflon inserts with a glass pipette. The Teflon containers were placed into the steel autoclaves and locked with a dynamometric key (60 kN). Sample codes, autoclave numbers, sample weights, temperatures and experimental durations are given in Tab. 1 and 2 for experiments with and without Al^{3+}, respectively:

Sample #	Autoclave #	Diatomite (g)	Temperature (°C)	Duration (d)
Z36	16	0.5025	100	0,25
Z37	145	0.5010	100	1
Z38	77	0.5020	100	2
Z39	70	0.5023	100	4
Z40	126	0.5016	100	8
Z41	71	0.5017	100	16
Z42	170	0.5007	100	32
Z43	177	0.5003	100	64
Z44	8	0.5004	25	64

Table 1: Sample information for experiments with Al^{3+} ("a")

Sample #	Autoclave #	Diatomite (g)	Temperature (°C)	Duration (d)
Z45	116	0.5013	100	0,25
Z46	125	0.5027	100	1
Z47	136	0.5004	100	2
Z48	73	0.5004	100	4
Z49	100	0.5005	100	8
Z50	82	0.5002	100	16
Z51	75	0.5006	100	32
Z52	168	0.5008	100	64
Z53	145	0.5021	25	64

Table 2: Sample information for experiments without Al^{3+} ("b")

Eight of the nine steel autoclaves (Z36-Z43 and Z45 – Z52, respectively) were placed into a rotating oven (company Memmert) at a temperature of 100 °C.

Rotation was started after 6 h when the Teflon inserts were self-sealed due to heating, which was controlled by an external thermometer. The reference sample (Z44) was stored at room temperature (~25°C) during the experiment. After certain reaction times (Tab. 1 and 2) autoclaves were taken out of the oven, cooled down to room temperature for 2 h and opened with the dynamometric key. The pH was measured in the supernatant solution before vacuum filtration through a 0.45 µm nitrocellulose filter. The filter cake was rinsed with 200 ml MQ water, before it was dried at 40°C in a porcelain dish, weighted and stored in a glass tube. The experimental design is shown in Figure 3.1.

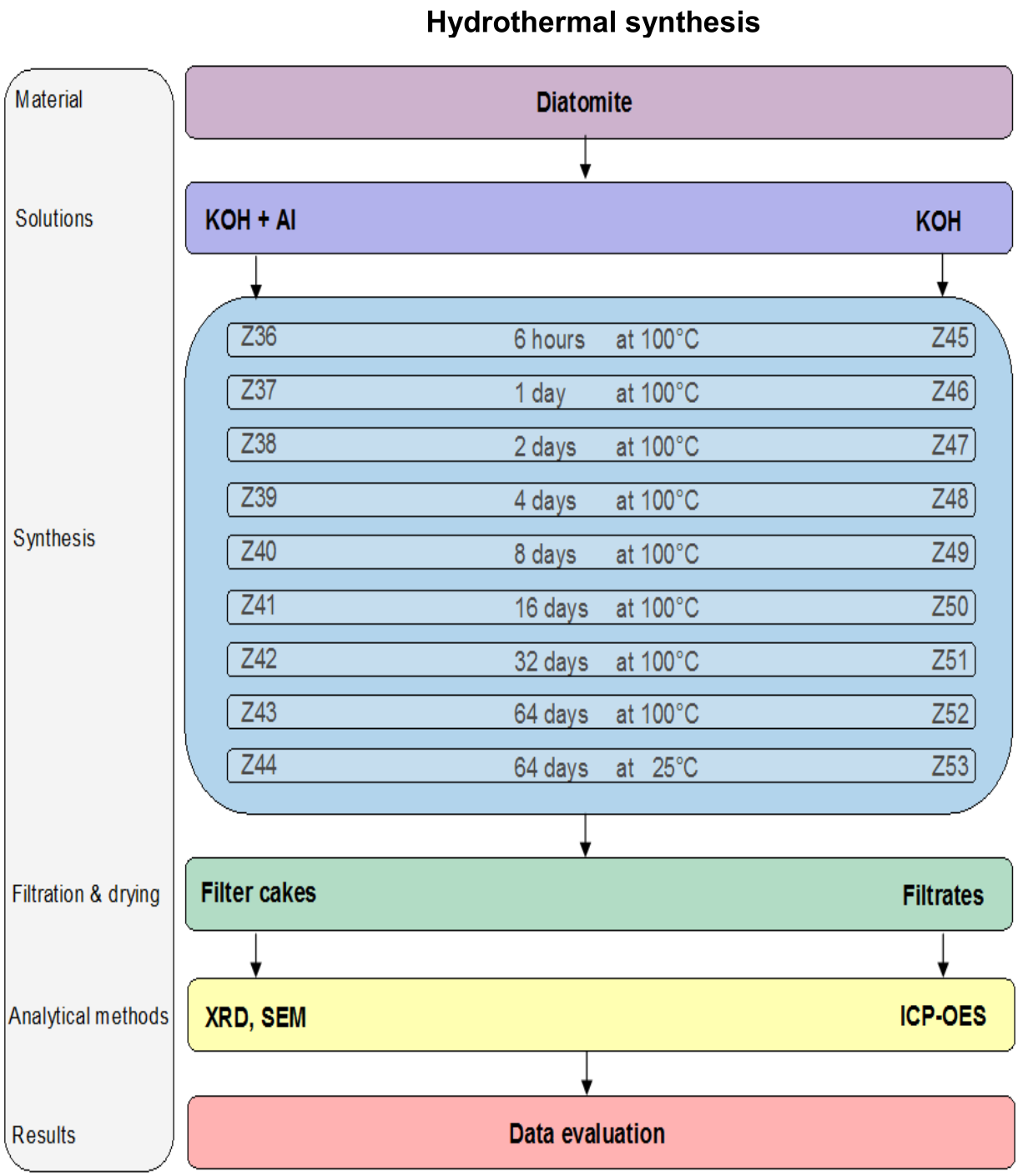

Fig. 3.1: Overview of diatomite alteration experiments

3.2 Metal removal experiments

0.05 g of every reaction product from diatomite alteration experiments were mixed in PP vials with 0.01 L of either the mine drainage solution or the synthetic heavy metal solution. The exact amounts of added solid are given in Tab. 3.

Sample #	Mine solution (mg)	Synthetic solution (mg)
Z36	50.7	50.9
Z37	52.2	50.8
Z38	50.4	51.0
Z39	50.7	51.3
Z40	50.2	50.7
Z41	50.0	51.0
Z42	50.1	50.0
Z43	50.8	50.0
Z44	50.9	51.2
Z45	51.2	50.9
Z46	51.3	50.1
Z47	50.1	51.1
Z48	51.2	51.0
Z49	50.7	50.3
Z50	50.9	50.2
Z51	50.5	50.1
Z52	50.1	50.9
Z53	51.3	50.1

Table 3: Weighted amount of the added solid in 0,01 L of mine drainage solution or synthetic heavy metal solution.

The mixtures were placed in a horizontal shaking device (E.B. KS-15) with a rotating frequency of 250 rpm. After 3 d reaction time at 25 °C the samples were filtrated using syringes with 0.2 µm filters. The filter cakes were dried in porcelain dishes at 40 °C and stored in glass tubes. The solutions were acidified with 200 µL conc. HNO_3 for ICP-MS analyses. Changes of pH have been separately observed with 50 mg altered diatomite and 10 ml of the solutions through interval of 1 minute and 1 hour. The amounts of added solid are given in Tab. 4:

Sample #	Mine solution (mg)	Synthetic solution (mg)
Z00	50.3	51.0
Z36	50.6	50.3
Z39	50.1	49.8
Z43	50.6	50.8
Z45	50.8	50.8
Z48	29.8	-
Z52	50.7	37.6

Table. 4: Weighted amount of the added solid in 0,01 L of mine drainage solution or synthetic heavy metal solution. Z00 represents non-altered diatomite.

4 Results

4.1 Alteration experiments

4.1.1 Solution chemistry

Alteration of diatomite leads to a decrease of the pH from almost 13 to values between 11 and 11.5 both with and without Al^{3+}(Fig. 4.1):

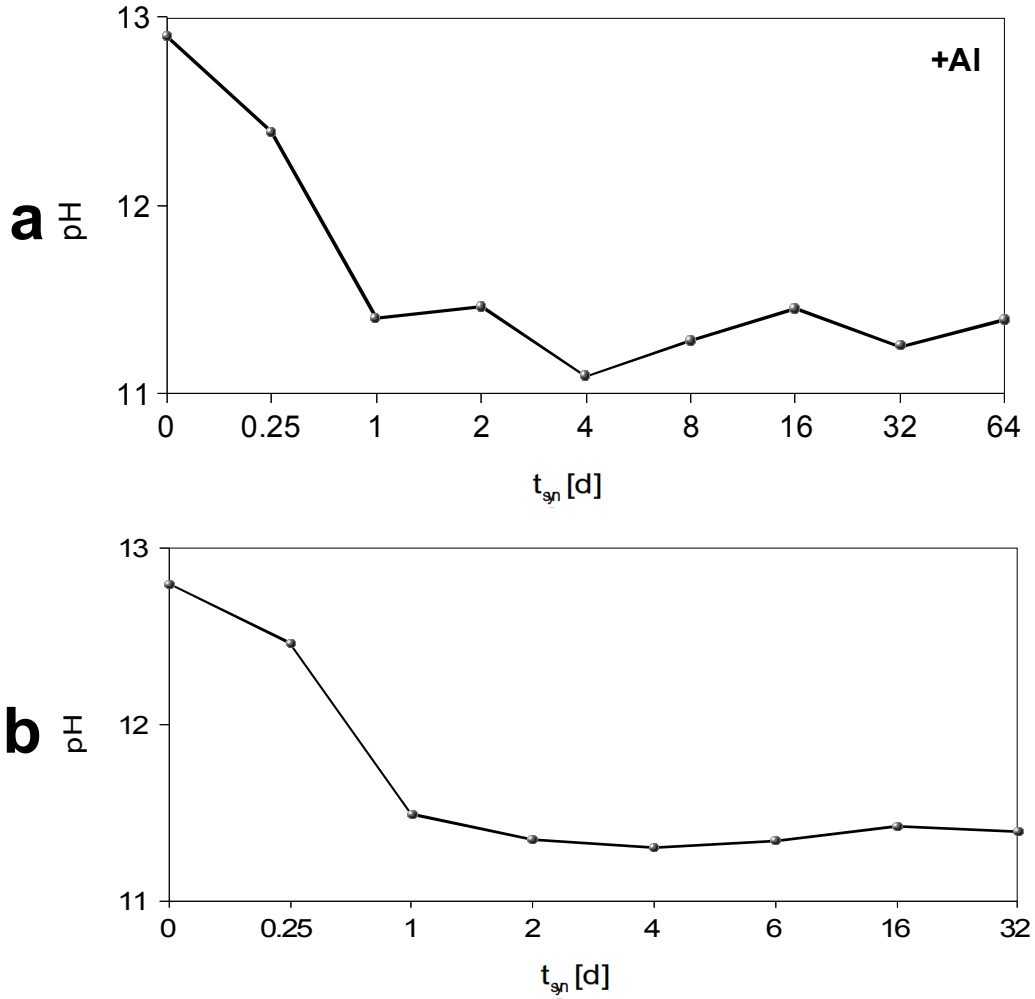

Fig. 4.1: pH as a function of time of synthesis (t_{syn}) for experiments with and without Al^{3+}("a" and "b", respectively)

In all diatomite alteration experiments – with and without Al^{3+} - the potassium concentration decreases slowly from about 3.5 gL^{-1} to about 2.9 gL^{-1}. Interestingly, the concentration decreases faster for experiments without Al^{3+}. Contrarily, silica concentrations increase in both experimental series within 1 d from zero to 1.6 gL^{-1}. Interestingly, in experiments with Al^{3+} the Si^{4+} concentration decreases slightly to 1.3 gL^{-1} whereas in experiments without Al^{3+} it increases further to more than 2.5 gL^{-1}. In the experimental series with Al^{3+}, about 90 % of this element is already consumed within the first 6 h. Finally, no significant amounts of Al^{3+} remain in solution (Fig. 4.2):

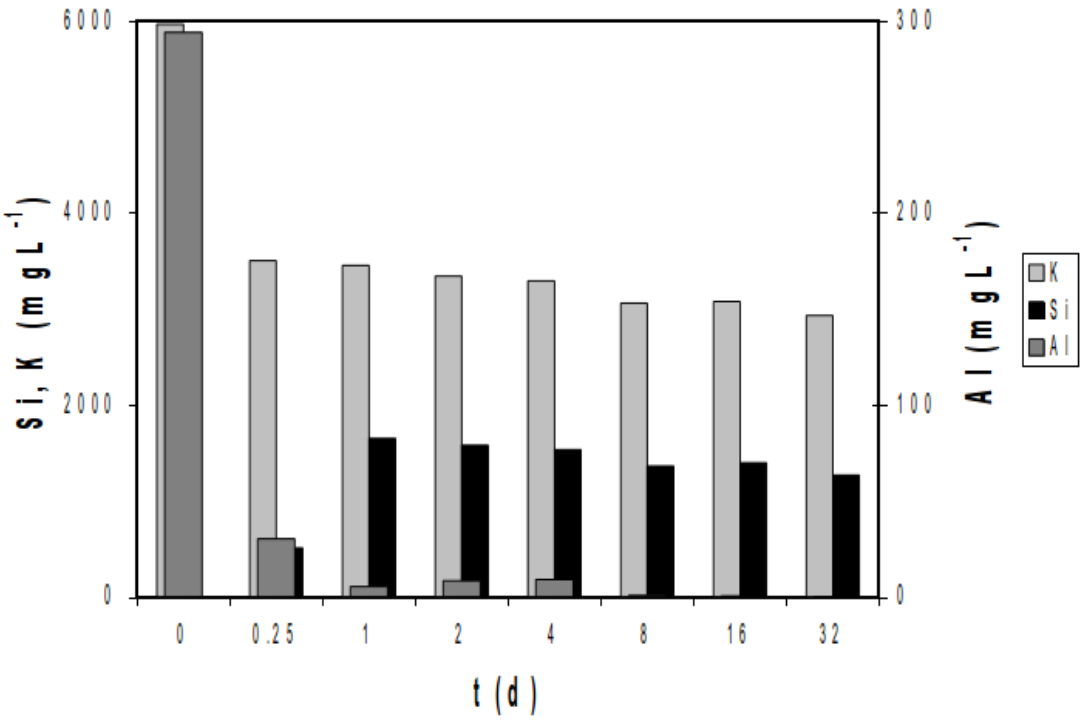

Fig. 4.2: Evolution of concentration of K^+, Al^{3+} and Si^{4+}. Through the experimental run with Al^{3+}.

4.1.2 Alteration product

In the alteration experiments with and without Al^{3+} an amorphous phase appears (Fig. 4.3 and Fig. 4.7 “b”). Since an amorphous particular phase forms also in the same experimental setting but with 1 M KOH instead of 0.1 M KOH **(*Höllen, 2012*)** when its formation is followed by the crystallization of the zeolite merlinoite, this phase is termed “intermediate phase” (IP). It is described as an amorphous, potassium-rich hydroxy-aluminosilicate. The morphological diversity of the IP is displayed in Fig. 4.3.

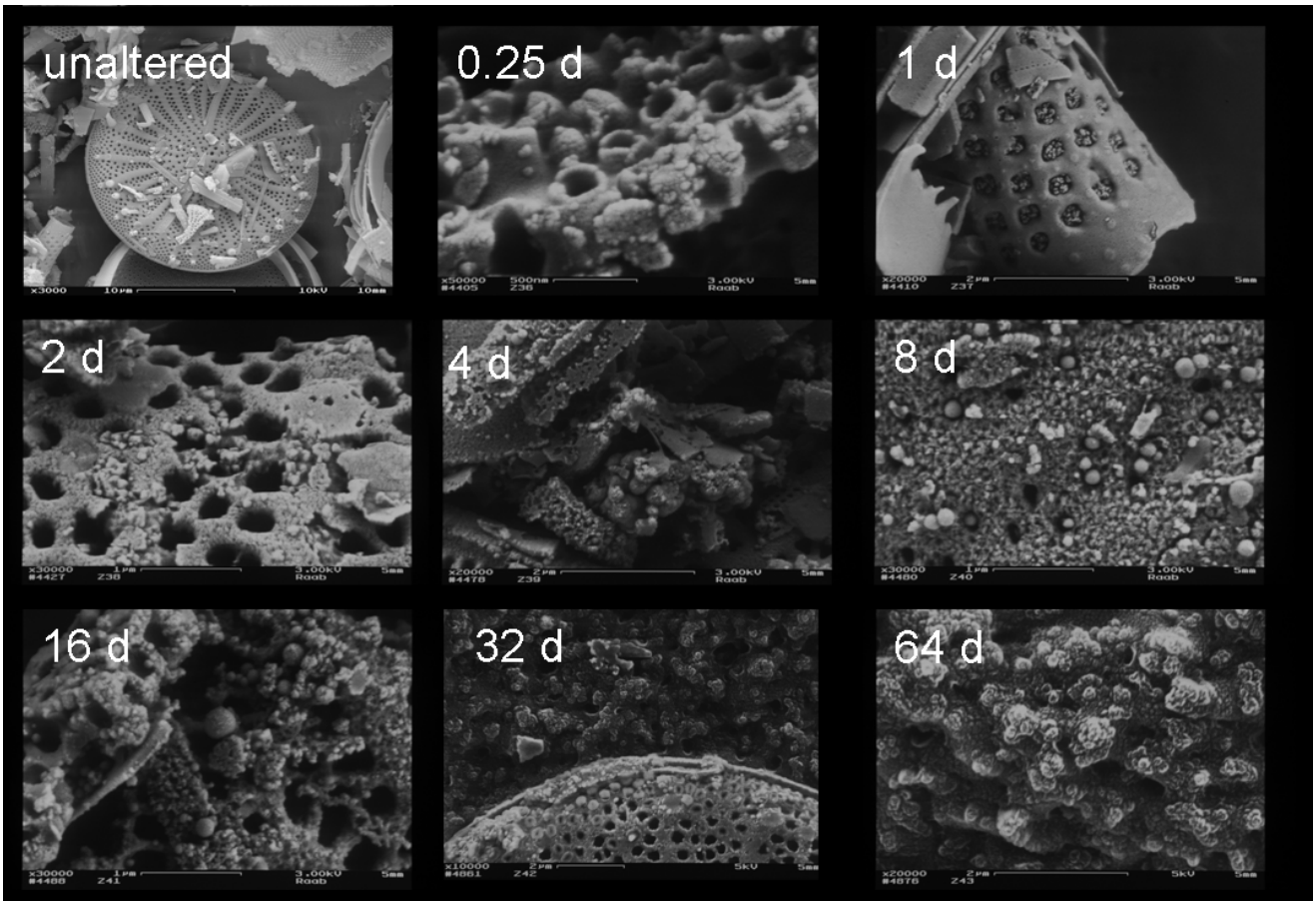

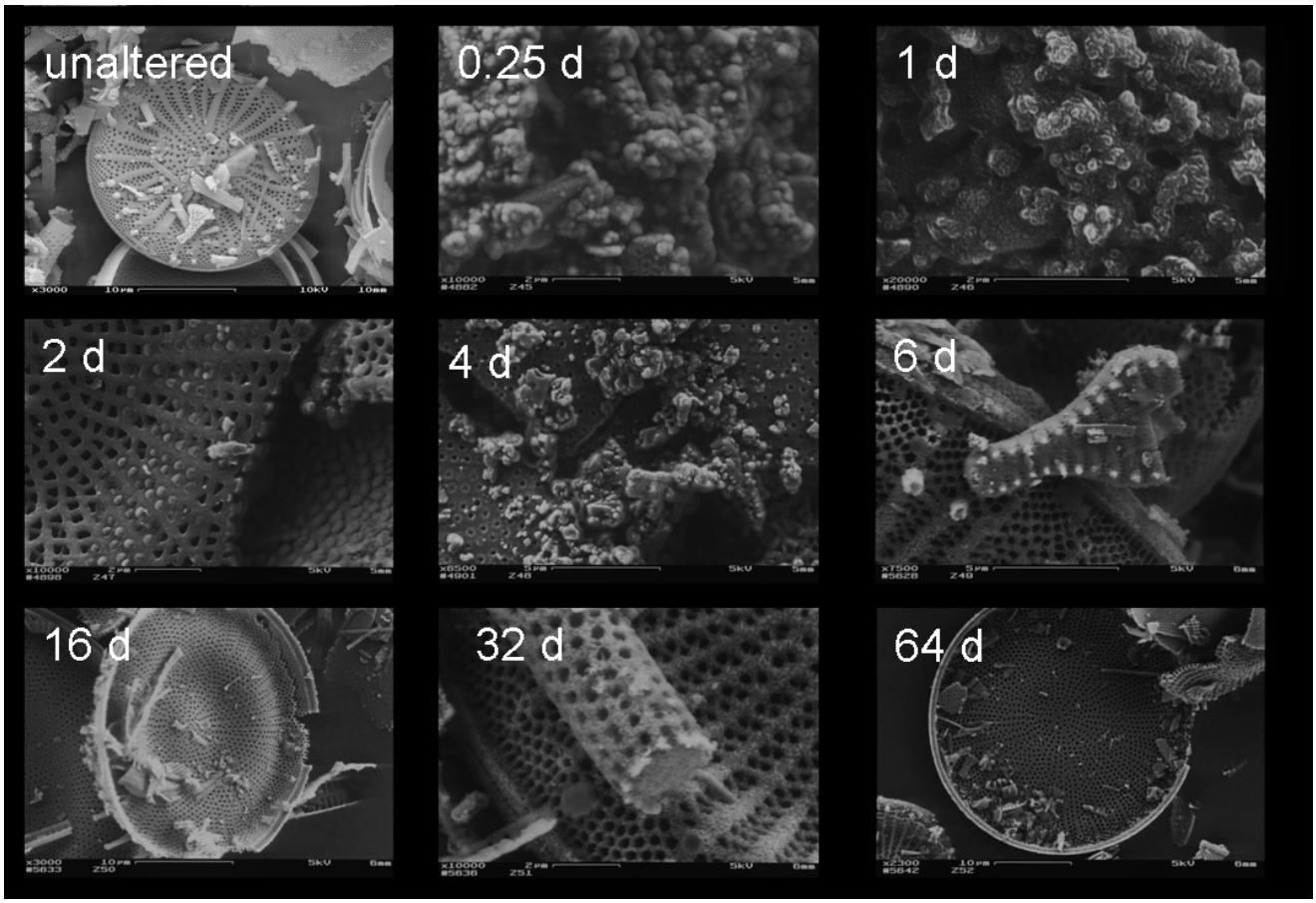

Fig. 4.3: SEM-SE images of diatomite altered in 0.1 M KOH at 100 °C after various alteration times (0.25 d ≤ t_{syn} ≤ 64 d). „a“ = with Al^{3+}; „b“ = without Al^{3+}

Comparing the reaction products in the experiments with and without Al^{3+} yields in several similarities and differences:

(i) An IP occurs in both experiments at 0.25 d alteration time but the morphology is different. In case of the experiment with Al^{3+} it appears as few irregularly shaped particles which are attached to the diatom and form clusters around the pores. Contrarily, in experiments without Al^{3+} occur aggregates of spherical particles of about few hundred µm diameter (Fig. 4.3).

(ii) In the alteration experiments with Al^{3+} after 8 d the attachment of spherical particles of about 100 – 200 nm diameter to the altered diatom surface is observed. However, it is important to note that the pores of the diatoms are mostly still open.

(iii) After 16 d a high amount of the IP can be seen in the alteration experiment with Al^{3+} (Fig. 4.3; “a”). Interestingly, even after 32 d nearly unaltered diatoms are present in the experiment without Al^{3+} (Fig. 4.3; “b”).

(iv) In the experiment without Al^{3+} also an IP is formed. Furthermore the surface is covered with nano-particles and the diatom surface is altered (Fig 4.4).

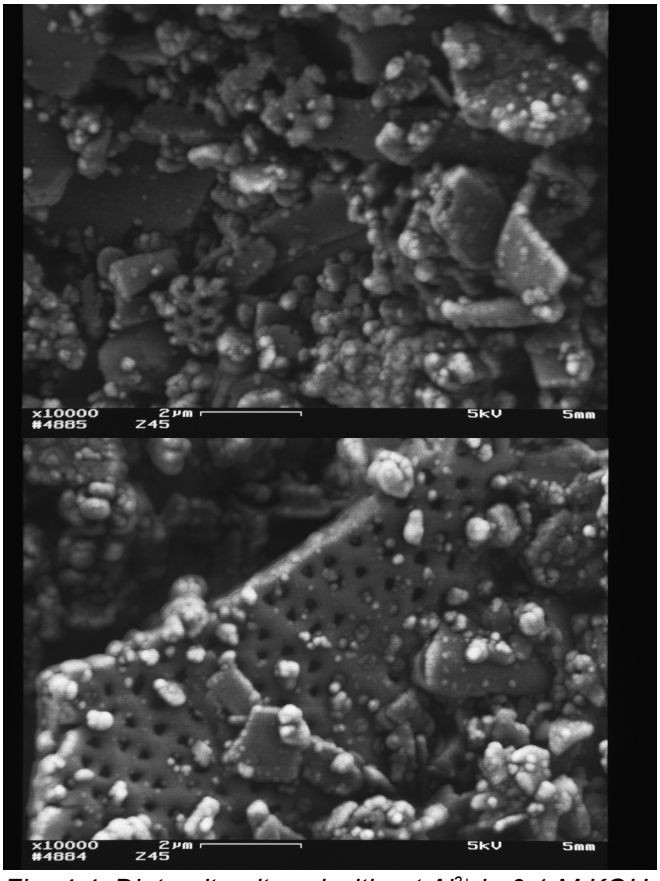

Fig. 4.4: Diatomite altered without Al^{3+} in 0.1 M KOH at 100°C for 0.25 d showing the intermediate phase (IP) attached to a diatom´s surface. (Fig.3.1; “b”)

However, there are still many unaltered diatoms coexisting. Interestingly after 2 d the amorphous IP is restricted to few pores within certain diatoms (Fig. 4.5). Most diatoms are unaltered (Fig. 4.6).

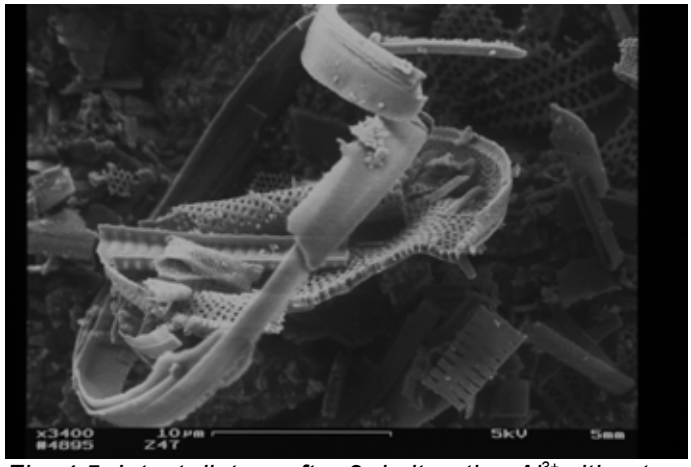

Fig. 4.5: Intact diatom after 2 d alteration Al^{3+} without (Fig. 3.1; "b")

(v) After 6 d of alteration without Al^{3+} there are still only few nano-particles, the surface is even less altered than for the samples altered without Al^{3+} for 0.25, 1, 2 or 4 d. After 16 d no alteration at all is observed. The pores are perfectly shaped. The IP was not found.

(vi) After 32 d only slight alteration of the surface of the experiments without Al^{3+} could be seen which was much less pronounced as for samples altered for 4 d or less. Even after 64 d nearly unaltered diatoms dominate the sample and their surfaces do not indicate a strong alteration.

(vii) The reference sample, which was altered at room temperature for 64 d, traces alterations but these are not very significant. Fig. 4.6 displays a diatom with closed pores, but no further alteration has been found.

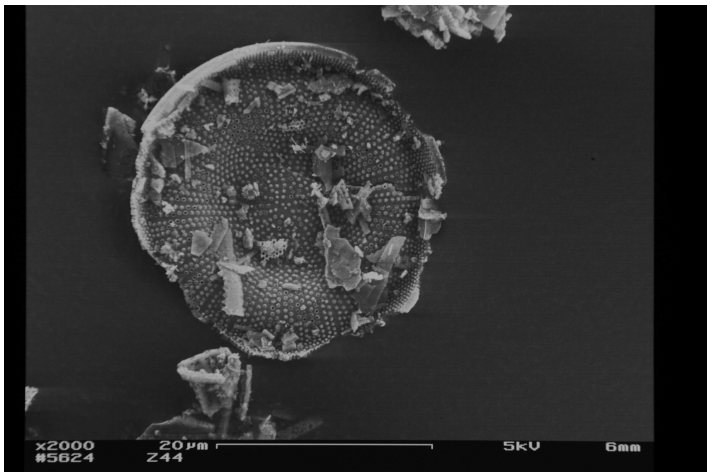

Fig. 4.6: Diatomite altered at room temperature (~25°C) for 64 d with Al^{3+} (Fig. 3.1; "a")

(viii) As the most important observation can be said that the Al^{3+} obviously serves as a stabilizer for the IP.

4.1.3 Mineralogical changes of the diatomite

X-ray diffraction patterns do not show any significant difference between the altered samples and the unaltered diatomite (Fig. 4.7). Quartz is the only crystalline phase in the diatomite and is indicated by the (101) peak at 3.34 Å or 31.1 °2Θ, respectively. All other peaks are result from zinc oxide which was added as an internal standard (Fig. 4.7).

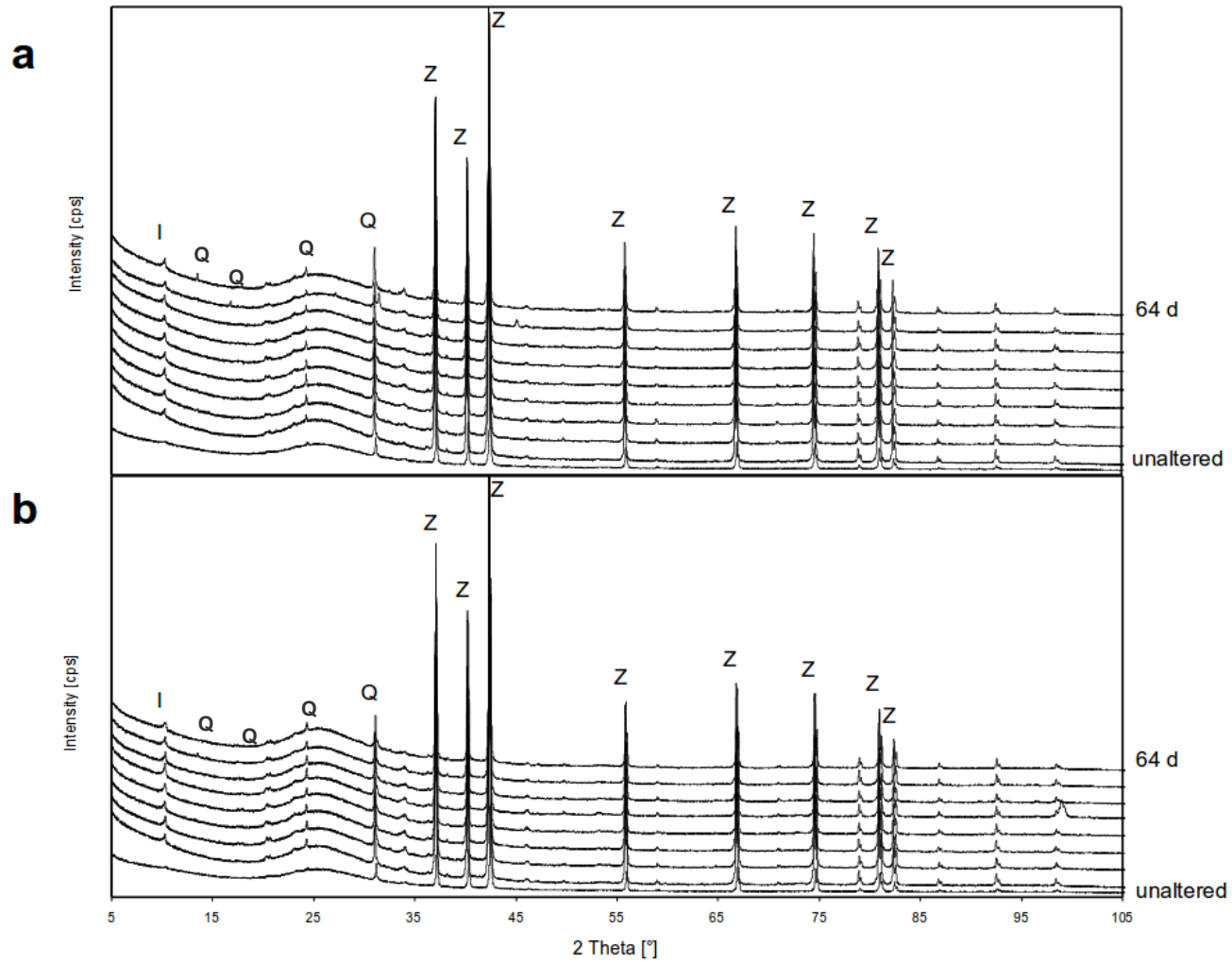

Fig. 4.7: XRD patterns of diatomite altered for various durations in 0.1 M KOH at 100 °C with and without Al^{3+} ("a" and "b", respectively) showing illite (I), quartz (Q) and the internal standard zincite (Z)

Rietveld refinement shows that unaltered diatomite consists of 97 wt-% amorphous phase, 2 wt-% mica and 1 wt-% quartz. Since no other phases are formed and the intensity of the quartz peak does not increase over time it can be concluded that the samples remain predominantly amorphous.

4.2 Metal removal experiments

4.2.1 Synthetic metal ion solution

Unaltered diatomite is not able to remove Pb^{2+} from the synthetic aqueous solution (Fig. 4.8). However, hydrothermal alteration creates a capacity to remove Pb^{2+} from an aqueous solution. Pb^{2+} removal is more efficient (up to 99 %) with the presence of Al^{3+} at the synthesis. In absence of Al^{3+} it only accounts for 40 to 70 %. In this case diatomite altered for intermediate periods (4 d) possesses the highest Pb^{2+} removing capacity. In contrast to Pb^{2+}, even unaltered diatomite can remove 20 % of dissolved Cu^{2+} from the synthetic solution. But also for Cu^{2+} the metal removal capacity can be increased by hydrothermal alteration, namely to 40 % without Al^{3+} and even to 60 % with the presence of Al^{3+} during the synthesis. Zn^{2+} is only removed to a very limited degree (10 – 20 %) from the synthetic solution even by altered diatomite. The order of selectivity of heavy metal removal from the synthetic solution is therefore $Pb^{2+} > Cu^{2+} > Zn^{2+}$ for both experiments with and without Al^{3+}.

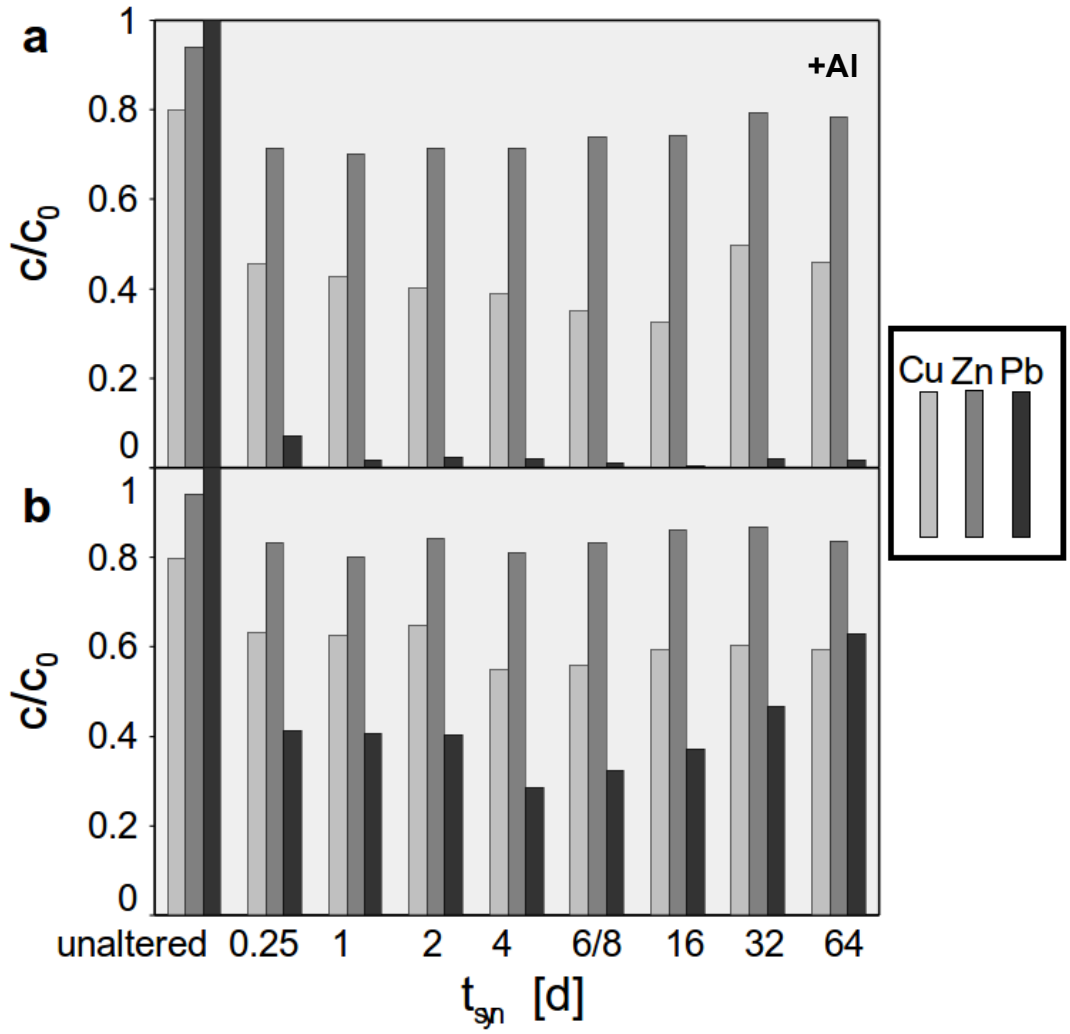

Fig. 4.8: Removal of Cu^{2+}, Zn^{2+} and Pb^{2+} from a synthetic solution after 3 d of reaction with diatomite altered hydrothermally for various durations with and without Al^{3+} ("a" and "b", respectively). The initial concentration (C_0) is set in ratio with the final concentration (C) for comparability.

4.2.2 Mine drainage solution

Since Cu^{2+} concentrations in the mine drainage solution are low, Cd^{2+} is investigated instead so that Cd^{2+}, Zn^{2+} and Pb^{2+} are compared (Fig. 4.9). Heavy metal removal from the mine drainage solution is more efficient than from the synthetic solution which had much higher initial ion concentrations. Contrary to the experiments with the synthetic solution even unaltered diatomite can remove about 50 % of Zn^{2+} and 95 % of Pb^{2+} from the mine drainage solution. Interestingly, diatomite altered without the presence of Al^{3+} was more capable of removing heavy metals than diatomite altered with presence of Al^{3+}. In contrast to experiments with the synthetic solution, Zn^{2+} is favoured for fixation by altered diatomite compared to Pb^{2+}. Cd^{2+} shows an intermediate behaviour. Generally, the duration of alteration had no impact on the capacity of heavy metal removal.

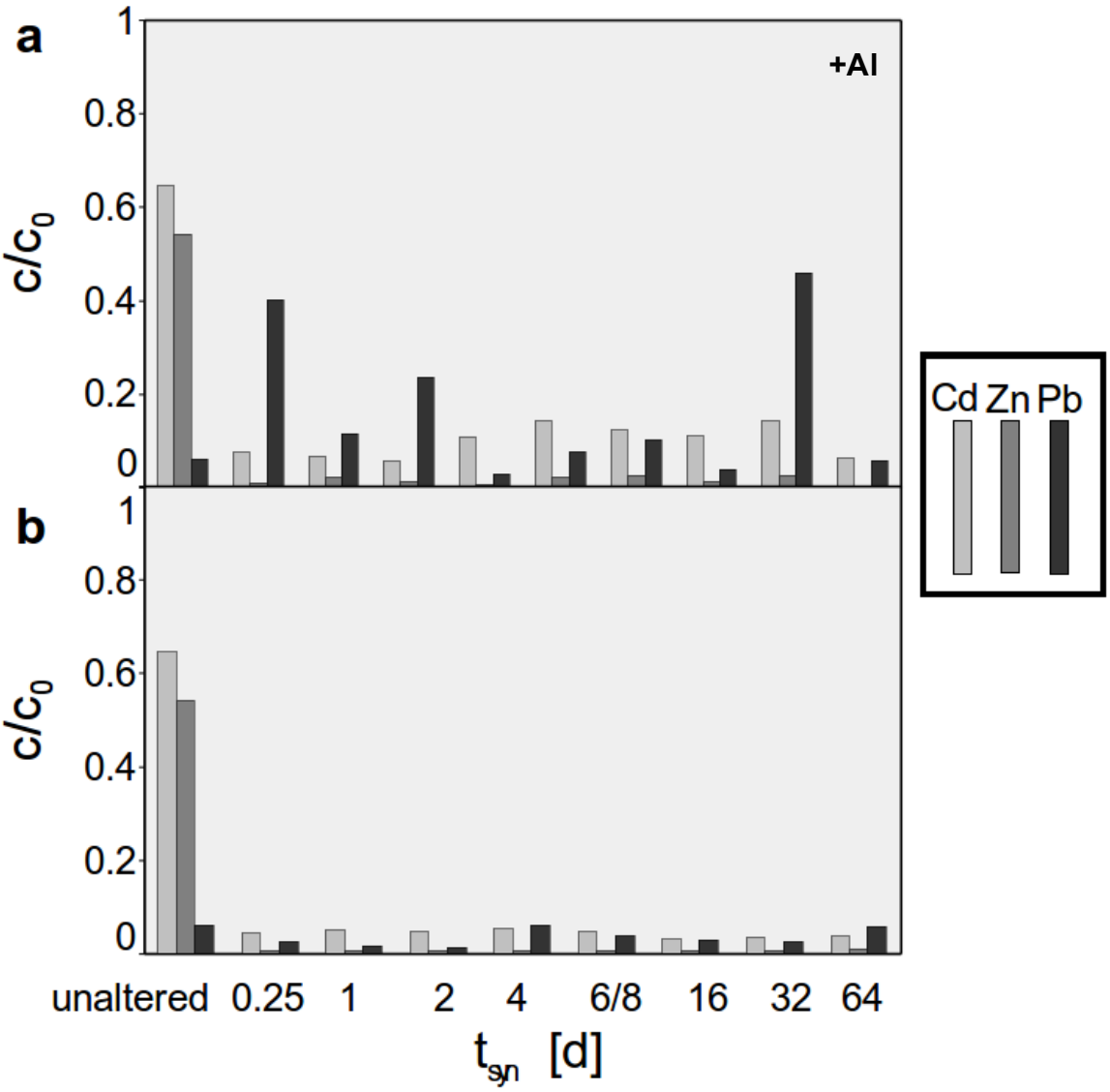

Fig. 4.9: Removal of Cd^{2+}, Zn^{2+} and Pb^{2+} from a mine drainage solution after 3 d of reaction with diatomite altered hydrothermally for various durations with and without Al^{3+} ("a" and "b", respectively). The initial concentration (C_0) is set in ratio with the final concentration (C) for comparability.

4.2.3 Evolution of pH through ion exchange experiments

The changes of the pH of the solutions have been separately observed by using selected samples (Tab. 4).

1) For the metal fixation experiments from mining water, the pH constantly remains at 8.2 by the use of unaltered diatomite (Z00), while it rises during the use of hydrothermally altered diatomite with or without Al^{3+} to 8.5 +/- 0.1. This can be explained by the release of hydroxide ions by the dissolution of altered diatomites.

2) However in the metal experiments from fixation synthetic heavy metal solutions, the pH changes also during the use of unaltered diatomite from 4.3 to 5.3. This can be explained by the low pH of the solution through the release of lower proportion of OH^- ions in the unaltered diatomite. However, the pH increase occurs also less pronounced than by using altered diatomite, it increases the pH to 5.7 +/- 0.1.

5 Discussion

The results of the alteration experiment revealed that the pH decreased (Fig. 4.1) in both sets of the experiment, regardless of the presence of Al^{3+}. The reason for this similar decrease is the solubility of Si^{4+} as function of the pH and temperature (***Amjad, 1998***). Because of the high pH of the system a large amount of Si^{4+} dissolves. The Si^{4+} binds the OH^- ions to form $Si(OH)_4$ molecules and through the removal of OH^- ions the pH decreases. The high solubility of amorphous silica can be explained by the elevated temperature of 100°C. The decrease of K^+ and Al^{3+} concentration (Fig. 4.2) is caused by the formation of an intermediate phase (IP), which contains these both elements besides Si^{4+} (Fig. 4.3). In none of the conducted experiments zeolites have been formed. In a similar experiment with 1 M KOH instead of 0.1 M KOH (***Höllen, 2012***) merlinoite has been formed. The KOH concentration is suggested to be too low for zeolite formation and so only the IP (Fig. 4.3) has been formed. After 6 d the IP starts to disappear in the diatomite without Al^{3+}. This means that incorporated Al^{3+} stabilizes the IP. The re-dissolution of the IP in the experiment without Al^{3+} after 6 d is not only seen in SEM-SE images (Fig. 4.3) but also by the rise of Si^{4+} concentration (4.1.1). In contrast a constant amount of the IP was present in diatomite altered up to 64 d in the presence of Al^{3+}. Therefore it appears that Al^{3+} stabilises the IP, because after 6 d of hydrothermal treatment without Al^{3+} the content of IP decreases continuously (Fig. 4.1).

The reason of the excellent removal of Pb^{2+} from the synthetic aqueous solution could be caused by the increased surface of the diatomite through the IP, and the presence of Al^{3+}. The reason for the higher removed amount of metal ions in the mine solution compared to the synthetic solution, could be the reaching of capacity limits of the alteration products at the synthetic solution because of the high concentration of metal ions. The reaction products of the metal removal experiment with and without Al^{3+} have the same selectivity order of $Pb^{2+} > Cu^{2+} > Zn^{2+}$ which is the same order as it is for the dehydration energy, beginning with Pb^{2+} as the lowest ***(Lee, 2011)***. Therefore Pb^{2+} is preferably fixed regardless of the presence of Al^{3+}. The diatomite altered with an Al^{3+} containing solution is better suitable for the higher concentration and lower pH setting of the synthetic solution experiment (Fig. 4.8) while the diatomite altered with an Al^{3+} free solution is better usable for the lower concentration and higher pH setting of the mine drainage solution experiment (Fig. 4.9). The fixation of Al^{3+} during the alteration creates a negatively charged surface which can bind heavy metal ions even if a low pH decreases the surface charge, if the concentration of the heavy metal ions is high enough. When Al^{3+} is missing during the alteration the surface is neutral and a high pH is needed to create a negative charge with the OH^- to bind heavy metal ions.

6 Conclusions

Our experimental results show that hydrothermal alteration of diatomite at 100 °C in 0.1 M KOH does not lead to the formation of zeolites. Instead an x-ray amorphous “intermediate phase” (IP) occurred. During the reaction time the pH of the solutions (Fig. 4.1), K^{+} and Al^{3+} concentration decrease, while the Si^{4+} concentration increases (Fig. 4.2). The IP subsequently decomposes in the alteration experiments without Al^{3+}, but remains metastable in experiments with Al^{3+}.

Hydrothermally altered diatomite can remove efficiently and selectively heavy metal ions from synthetic and natural aqueous solutions in the order of $Pb^{2+} > Cu^{2+} > Zn^{2+}$. Diatomite alteration with Al^{3+} added to the KOH solution yields products suitable for heavy metal removal from highly polluted and acidic waters whereas alteration without additional Al^{3+} yields products which can be applied especially for weaker contaminated alkaline waters.

The hierarchical structure of the altered diatomite with and without Al^{3+}, and the combination of diatom macro-structure and IP ion exchange capacities are promising for waste water treatment.

Literature

R. Allmann, 2002, Röntgenpulverdiffraktometrie: Rechnergestütze Auswertung Phasenanalyse und Strukturbestimmung, 2nd ed., 7-38 p., Springer, Berlin

Z. Amjad, 1998, Water-soluble Polymers: Solution Properties and Applications, 174 p., Springer

G. Bignot, 1985, Elements of Micropalaeontology, Graham and Trotman, London

D.L. Bish and D.W. Ming, 2001, Natural Zeolites: Occurrence Properties Applications, Reviews in Mineralogy and Geochemistry, Vol. 45, Mineralogical Society of America, Washington

T.L. Brown, H.E. LeMay and B.E. Bursten, 2011, Chemie: Studieren kompakt, 10th ed., 646 p., Pearson, München

J.L. Goldstein and D.E. Newbury, 1997, Scanning Electron Microscopy and X-Ray Microanalysis: A Text for Biologists Materials Scientists and Geologists, 2nd ed., Kluwer Academic Publishers

D. Höllen, 2012, “Formation and Use of Amorphous Silica” PhD thesis. Graz University of Technology.

A. Jawor, B.H.Jeong and E.M.V. Hoek, 2009, Synthesis characterization and ion-exchange properties of colloidal zeolite nanocrystals, Journal of Nanoparticle Research, Volume 11, No 7, An Interdisciplinary Forum for Nanoscale Science and Technolog, Springer

S.S. Lee and K.L. Nagy, 2011, Heavy metal sorption at the muscovite (001)-fulvic acid interface, Environmental Science and Technology, 45 (22), 9574-9581 p.

J.H. Lipps, 1993, Fossil Prokaryotes and Protists, Blackwell Scientific Publishers, Boston & Oxford

A. Moirou, A. Vaxevanidou, I. Paspaliaris and G.E. Christidis, 2000, Ion Exchange of Zeolite Na-Pc with Pb^{2+} Zn^{2+} and Ni^{2+} Ions, Clays and Clay Minerals, Vol. 48, No 5, 563-571 p.

T. Motsi, N.A. Rowson, M.J.H. Simmons, 2009, Adsorption of heavy metals from acid mine drainage by natural zeolite, Int. J. Miner. Process., 92, 42-48 p.

M. Okrusch and S. Matthes, 2009, Mineralogie: Eine Einführung in die spezielle Mineralogie, Petrologie und Lagestättenkunde, 8th ed., Springer, Heidelberg

D.L. Parkhurst and C.A.J. Appello, 1999, User's guide to PHREEQC (version 2): „A computer program for speciation, batch-reaction, one-dimensional transport and inverse geochemical calculations“,99-4259, 312 p., U.S. Geological Survey Water-Resources Investigations Report

D.A. Skoog and J.J. Leary, 1996, Instrumentelle Analytik: Grundlagen Geräte Anwendung, 455-496 p., Springer, Berlin

J.P. Smol and E.F. Stoermer, 2010, The Diatoms: Applicaitons for the Evironmental and Earth Sciences, 2nd ed., Cambridge University Press, Cambridge

H.E. Taylor, 2001, Inductively Coupled Plasma-Mass Spectrometry: Practices and Techniques, J. Chem. Educ., 78 (11), 1465 p., Eastman chemical Company, Kingsport